

Investigation of Thermal Stresses in Silicon by Source Image Distortion

Gene J. Carron, L. K. Walford, and James A. Schoeffel

Citation: *Journal of Applied Physics* **40**, 2372 (1969); doi: 10.1063/1.1657996

View online: <http://dx.doi.org/10.1063/1.1657996>

View Table of Contents: <http://scitation.aip.org/content/aip/journal/jap/40/6?ver=pdfcov>

Published by the AIP Publishing

Articles you may be interested in

[Photoinduced and thermal stress in silicon microcantilevers](#)

Appl. Phys. Lett. **73**, 2319 (1998); 10.1063/1.121809

[Dislocations in thermally stressed silicon wafers](#)

Appl. Phys. Lett. **22**, 261 (1973); 10.1063/1.1654632

[Comparison of X-Ray Topography and Infrared Birefringence for Investigating Thermal Stresses in Silicon](#)

J. Appl. Phys. **38**, 3949 (1967); 10.1063/1.1709046

[A Sound Source for Investigating Microphone Distortion](#)

J. Acoust. Soc. Am. **11**, 219 (1939); 10.1121/1.1916027

[A Sound Source for Investigating Microphone Distortion](#)

J. Acoust. Soc. Am. **11**, 164 (1939); 10.1121/1.1902128

This is a promotional banner for Shimadzu spectrophotometers. It features the Shimadzu logo (a red circle with a white cross) and the text 'SHIMADZU Excellence in Science' in white on a red background. To the right, the text 'Powerful, Multi-functional UV-Vis-NIR and FTIR Spectrophotometers' is written in black. Below this, a paragraph states: 'Providing the utmost in sensitivity, accuracy and resolution for applications in materials characterization and nano research'. A bulleted list of applications is provided: Photovoltaics, Polymers, Thin films, Paints, Ceramics, DNA film structures, Coatings, and Packaging materials. At the bottom left, a red link says 'Click here to learn more'. On the right, four different models of Shimadzu spectrophotometers are shown: a small benchtop unit, a larger benchtop unit with a sample holder, a large floor-standing unit, and a very large floor-standing unit with a sample compartment.

Investigation of Thermal Stresses in Silicon by Source Image Distortion*

GENE J. CARRON, L. K. WALFORD, AND JAMES A. SCHOEFFEL

Research Division, McDonnell Douglas Corporation, St. Louis, Missouri 63166

(Received 9 December 1968)

The source image distortion (SID) technique has been used to measure the stresses produced by electron beam melting of small regions of single-crystal silicon wafers. Stress values thus calculated ($\sim 10^8 \text{ Nm}^{-2}$) agree with other worker's results for stress levels close to the fracture point for single-crystal silicon. For wafers which had fractured, no source image distortion was visible indicating the absence of stress in those wafers.

I. INTRODUCTION

Thermal stresses in silicon generated by electron beam heating have been the subject of several studies reported by two of the authors.¹⁻⁵ These studies have dealt with x-ray topography, infrared birefringence, and an analytical treatment of the stress areas. In this paper we report the results obtained in an investigation of such stresses by the method of source image distortion (SID) developed by Young and Wagner.⁶ They provide a complete description and geometrical analysis of the method in their paper so we limit ourselves to the bare essentials necessary for clarity. In the SID technique a line source from an x-ray tube is separated into multiple point sources by a soller slit placed normal to the line. The path of rays from each source can be bent or distorted by either tilts or spacing changes in a crystalline lattice set for Laue diffraction. It is the distortion in the source image pattern which when photographed provides us with data of interest.

The SID photograph may also include topographic information of limited quality. In this study, the four-lobed rosette patterns are superimposed on the SID patterns in some instances.

Our over-all purpose in applying the SID technique is to provide supplemental data to our previous investigations and to examine these results in connection with our proposed stress model for a resolidified electron beam spot. For the sake of comparison, we have used the same specimens as were used in the previous investigations whenever possible.

II. ANALYSIS

The following equations taken from Young and Wagner's paper were used to separate the strain and tilt effects. See Fig. 1 Laue geometry.

$$\beta = \theta + \alpha + \Delta\theta + \Delta\alpha, \quad (1)$$

* This research was conducted under the McDonnell Douglas Independent Research and Development Program.

¹ G. J. Carron and L. K. Walford, *Appl. Phys. Letters* **7**, 304 (1965).

² G. J. Carron, *Appl. Phys. Letters* **9**, 355 (1966).

³ G. J. Carron and L. K. Walford, *J. Appl. Phys.* **38**, 3949 (1967).

⁴ G. J. Carron and L. K. Walford, *J. Appl. Phys.* **39**, 3813 (1968).

⁵ L. K. Walford and G. J. Carron, *J. Appl. Phys.* **39**, 5802 (1968).

⁶ R. A. Young and C. E. Wagner, *J. Appl. Phys.* **37**, 4070 (1966).

where β = the angle between the incident beam and the normal to the crystal surface, α = angle measured in the plane of incidence between the diffracting plane and the crystal surface (symmetric case $\alpha = 0$), $\Delta\theta$ = change in angle due to strain, $\Delta\alpha$ = change in angle due to tilt; and

$$\Delta\beta = (\Delta S/L) \cos\theta, \quad (2)$$

where $\Delta\beta$ = measure of distortion, ΔS = shift in locus of reflection on the main face of the crystal in a direction perpendicular to the undisturbed locus.

Using data taken from the two reflections $\{111\}$ and $\{333\}$ for which the reciprocal lattice points lie on the same central line, we proceed

$$\Delta\theta = \epsilon \tan\theta. \quad (3)$$

For the strain effect

$$\epsilon = (S_2 - S_1)/(T_2 - T_1), \quad (4)$$

where $T = \tan\theta$, S_1 , S_2 are $\Delta\beta$ values for $\{111\}$ and $\{333\}$, respectively, and for the tilt effect

$$\Delta\alpha = S_2 - T_2(S_2 - S_1)/(T_2 - T_1). \quad (5)$$

III. EXPERIMENTAL

The apparatus used was similar to that employed by Young and Wagner. The line source of a CA-7 molybdenum target x-ray tube was separated into multiple sources by a 0.020-in. General Electric soller slit, 3.5 in. in length. This slit was positioned normal to the source and directly in front of the x-ray port. X-band waveguide was used as a collimating tube and a support for the soller slit and lineup slit. The source-to-specimen distance was 78 cm. A topographic camera was used for mounting the specimen because it provided all the necessary rotations and translations for alignment. The SID patterns were recorded on 3000 Polaroid 4×5 in., type 57 film, exposures normally being between 15 min and 1 h. However, in the case of highly perfect wafers the exposure was extended to several hours.

The specimens were single-crystal silicon wafers ranging in thickness from 0.010 to 0.020 in. The wafers had been processed in one or more areas by bombardment with a focused electron beam. This process melted the silicon in microspot areas which subsequently resolidified. It is the residual stresses induced in and around the beam spots during this processing which are under

study. Specimens were examined with the electron beam (E.B.) spots on the wafers positioned both toward the incident beam and away from the beam.

The experimental work was concentrated on wafers J, L1, and L2, designated as such in Ref. 3. Three electron beam spots are evident on wafers J and L1 all of which exhibited x-ray rosettes and/or birefringence under examination. Wafer L2 contained cleavage cracks surrounding the beam spots and exhibited neither x-ray rosettes nor infrared birefringence. SID patterns of these three wafers using both $\{111\}$ and $\{220\}$ reflections were recorded.

In order to obtain quantitative data on the magnitude of the internal stresses, SID photographs of wafer J, using $\{111\}$ and $\{333\}$ reflections were taken and enlarged. An electron beam spot was selected for analysis and the line positions from one side of the rosette figure to the other were measured. This was done in both the distorted and undistorted areas of the $\{111\}$ and $\{333\}$ SID patterns. Subtraction of one value from the other yielded a ΔS value for each line. The presence of the rosettes along with the SID pattern made it difficult to obtain accurate values, especially near the center of the pattern. The high intensity of the diffraction in this area masks the source image distortion. Another troublesome feature encountered in this wafer was the close proximity of the spots to each other which had to be taken into account in measurements of distortion. Equations (2), (4), and (5) were used to calculate strain and tilt values. Since silicon is reportedly anisotropic, a value of $1.86 \times 10^{11} \text{ N m}^{-2}$ ($1.9 \times 10^6 \text{ kg/cm}^2$) which corresponds to the $[111]$ direction, was used for Young's modulus to convert strain into stress.

Because the SID patterns were photographed directly on positive contrast Polaroid film the contrast in the SID patterns is reversed from topographs shown in previous reports.

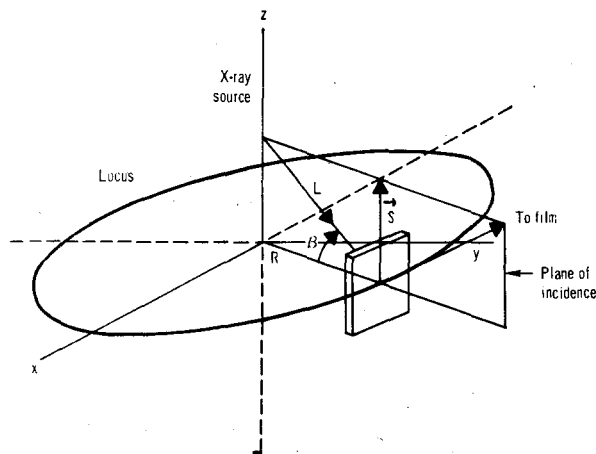


FIG. 1. SID geometry, Laue case.



FIG. 2. SID patterns of wafer J with electron beam spots positioned away from incident x-ray beam; shown here $\sim 10\times$. (a) $\{220\}$ reflection, (b) $\{111\}$ reflection.

IV. RESULTS

Figures 2(a) and 2(b) show the SID pattern obtained from $\{220\}$ and $\{111\}$ reflections, respectively, of wafer J when it is positioned with the E.B. spots on the face of the wafer away from the incident beam. Rosette patterns are superimposed on the SID pattern. The rosette configuration is identical to that obtained by Lang topography,³ and so, the SID technique is advantageous in that it permits an examination of the

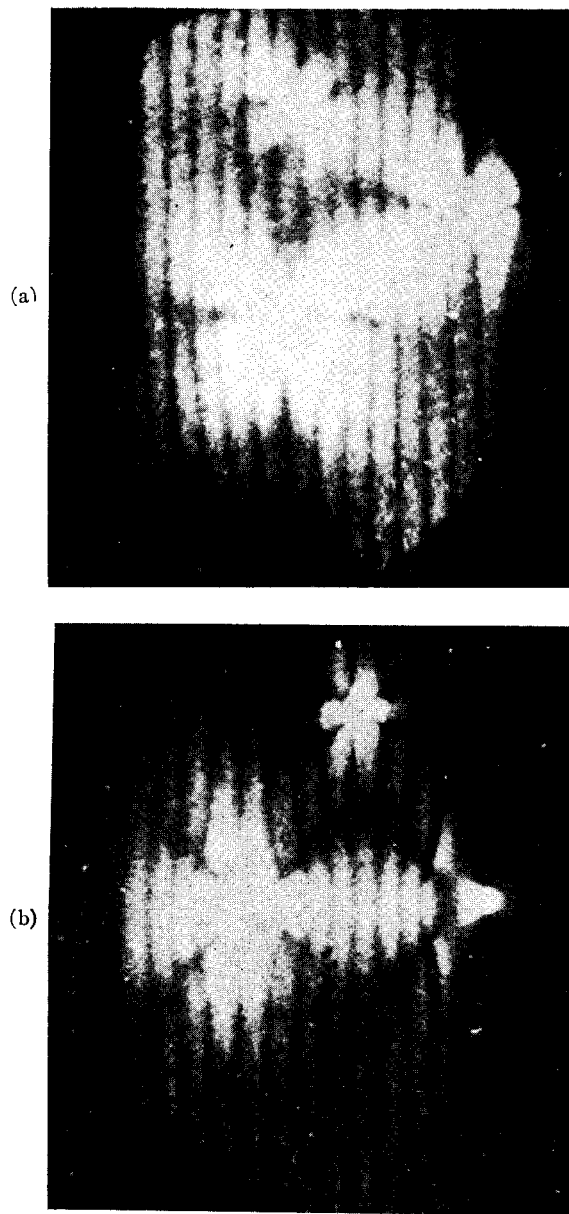


FIG. 3. SID patterns of wafer J with electron beam spots positioned toward the incident x-ray beam. $10\times$. (a) $\{220\}$ reflection, (b) $\{111\}$ reflection.

rosette patterns in the short exposure required. In both of these figures the source pattern is distorted by a bending of the image toward the center of the E.B. spots. These patterns should be compared with the SID patterns shown in Figs. 3(a) and 3(b). Once again these patterns were recorded using $\{220\}$ and $\{111\}$ reflections, but with the crystal positioned with the E.B. spots toward the incident beam. In these latter figures the source pattern is bent away from the center of the spot.

Young and Wagner have indicated that patterns such as those shown in Figs. 2(a) and 2(b) are due either to a convex tilt toward the beam or to a localized

strain gradient. Also, patterns such as those shown in Figs. 3(a) and 3(b) are indicative of a concave tilt toward the beam or a localized strain gradient of opposite sign.

Figure 4 shows a $\{220\}$ SID pattern of wafer L2 covering spots 4, 5, and 6, all of which exhibited cleavage cracks (see Fig. 5, Ref. 3). As stated previously the E.B. spots on this wafer showed neither x-ray rosette patterns nor infrared birefringence. The absence of strains or tilts in this wafer is confirmed by the undistorted SID pattern. The perfection of this wafer is manifested in the long exposure time (approximately 16 h) necessary to reveal a good SID photograph.

Several factors influence the recording of accurate deformation data. Among these are: the change in stress level with changes in electron beam parameters, the effect from adjacent electron beam spots, and the information lost at the center of the rosette as previously mentioned. Due to the last, more information can be obtained from patterns such as 3(a) and 3(b) where the deformation is away from the center of the spot. Measurements of ΔS taken on the electron beam spots on wafer J reveal that the stress level at the center of the spots ranges from $9 \times 10^7 \text{ N m}^{-2}$ to $1.5 \times 10^8 \text{ N m}^{-2}$. There is also a change in sign of the stress at the center of the spots. The stress level decreases linearly toward the outer edge of the rosette pattern to a

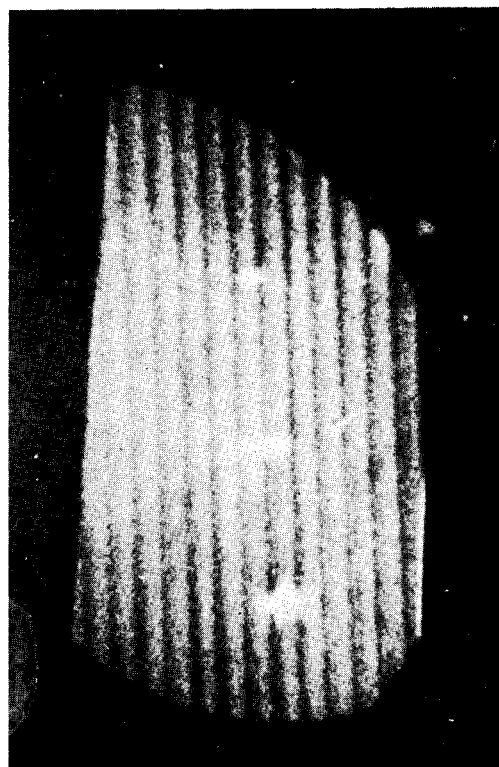


FIG. 4. Absence of distortion in SID pattern, $\{111\}$ reflection, of wafer L2. $10\times$.

value of $7 \times 10^7 \text{ N m}^{-2}$. This represents a change in strain of the order of 10^{-3} to 10^{-4} . Outside the rosette, the stresses appear to decrease very rapidly, but unfortunately, the technique is insensitive at this level. The SID patterns of wafer L1 indicate that the stress level in this wafer has decreased appreciably due to chemical etching of the surface in previous investigations.

These values are in good agreement with those reported in other studies on stresses in silicon. Pearson *et al.*,⁷ reported their maximum observable stress on small single crystals of silicon to be $5 \times 10^9 \text{ N m}^{-2}$, a value which corresponds to 2.6% elastic strain; they further stated that this may possibly be the fracture strength of a perfect crystal.

Dumin⁸ in studying the stress in epitaxial silicon films on single-crystal sapphire calculated the stresses in the films to be of the order of 10^8 – 10^9 N m^{-2} . He states that 10^9 N m^{-2} is the ultimate strength of silicon and that no cracking or breaking up of the films has been noticed. He further states that stresses of this order are sufficient to alter the mobility and resistivity of the films.

Giardini⁹ measured the stress-optical relationship in silicon up to stresses of approximately $4.5 \times 10^7 \text{ N m}^{-2}$. Billig¹⁰ calculates that the thermal strain in rapidly cooled crystals is of the order of 3×10^{-4} , which corresponds to a stress of 10^7 N m^{-2} . This, he points out, is of the same order of magnitude as the yield point of many monocrystalline metals, 10^7 N m^{-2} . Penning,¹¹ in his study of germanium, states that Ge is extremely brittle below 400°C and fracture by cleavage along

a {111} plane usually occurs if the tension in the crystal exceeds $2 \times 10^8 \text{ N m}^{-2}$.

The values for lattice tilt, calculated from the SID photographs, ranged from 0.5 min near the edge of the rosette to 3.0 min at the center. We believe that these values account for the insensitivity of the back-reflection Laue technique used in previous experiments to detect lattice damage.

The wafers on which cement had been dried showed a similar reversal of distortion, depending upon the position of the cement relative to the incident beam; that is, whether or not the beam was toward or away from the cement.

V. DISCUSSION

From the foregoing data we can conclude that electron beam melting and the subsequent resolidification of single-crystal silicon can result in the development of residual stresses which lie in the upper range of the plastic region. The SID technique permits calculation of the stresses and lattice tilts in such resolidified areas if we assume the applicability of elastic theory. The calculated stress levels are in accord with the results reported by different investigators who have used other techniques. They also agree with our proposed stress model,^{4,5} in particular, in indicating a change of sign across the center of the beam spot. This follows from our prediction of a macrostacking fault based on the fast growth directions of a faulted lattice. If one considers the stress interactions due to nearest neighbors in such a model, a change in the sign of the stresses is plausible.

In those cases which approach or exceed the 10^9 N m^{-2} stress level, the stresses are relieved by cleavage along the {111} planes. This is evidenced not only by the cleavage cracks, but also by the absence of x-ray rosettes, infrared birefringence, and source image distortion.

⁷ G. L. Pearson, W. T. Read, Jr., and W. L. Feldmann, *Acta Met.* **5**, 181 (1957).

⁸ D. J. Dumin, *J. Appl. Phys.* **36**, 2700 (1965).

⁹ A. A. Giardini, *Am. Mineralogist* **43**, 249 (1958).

¹⁰ E. Billig, *Proc. Roy. Soc. (London)* **235**, 37 (1956).

¹¹ P. Penning, *Philips Res. Rept.* **13**, 79 (1958).